

those antibodies whose catalytic efficiency is less than that predicted on the basis of the available binding energy). Provided that our conjecture is correct about the structural limitations imposed on the catalytic antibody by the very nature of its induction, methods that focus on altering not only the identities but also the presentation of catalytic residues may offer a powerful means of evolving such initial catalysts to higher activities; in so doing, we will learn more about enzymes. □

Received 16 January; accepted 11 April 1995.

1. Stewart, J. D., Liotta, L. J. & Benkovic, S. J. *Acc. Chem. Res.* **26**, 396–404 (1993).
2. Stewart, J. D. & Benkovic, S. J. *Chem. Soc. Rev.* **22**, 213–219 (1993).
3. Lerner, R. A., Benkovic, S. J. & Schultz, P. G. *Science* **252**, 659–667 (1991).
4. Li, T., Janda, K. D., Ashley, J. A. & Lerner, R. A. *Science* **264**, 1289–1293 (1994).
5. Cravatt, B. F., Ashley, J. A., Janda, K. D., Boger, D. L. & Lerner, R. A. *J. Am. chem. Soc.* **116**, 6013–6014 (1994).
6. Na, J., Houk, K. N., Shevlin, C. G., Janda, K. D. & Lerner, R. A. *J. Am. chem. Soc.* **115**, 8453–8454 (1993).
7. Gouverneur, V. E. et al. *Science* **262**, 204–208 (1993).
8. Wolfenden, R. A. *Rev. Biophys. Bioengng* **5**, 271–306 (1976).
9. Benkovic, S. J., Napper, A. D. & Lerner, R. A. *Proc. natn. Acad. Sci. U.S.A.* **85**, 5355–5358 (1988).
10. Jacobs, J. W. *BioTechnology* **9**, 258–262 (1991).
11. Jackson, D. Y., Prudent, J. R., Baldwin, E. P. & Schultz, P. G. *Proc. natn. Acad. Sci. U.S.A.* **88**, 58–62 (1991).
12. Stewart, J. D., Roberts, V. A., Thomas, N., Getzoff, E. D. & Benkovic, S. J. *Biochemistry* **33**, 1991–2003 (1994).
13. Posner, B., Smiley, J., Lee, I. & Benkovic, S. *Trends biochem. Sci.* **19**, 145–150 (1994).
14. Stewart, J. D. et al. *Proc. natn. Acad. Sci. U.S.A.* **91**, 7404–7409 (1994).
15. Hirschmann, R. et al. *Science* **265**, 234–237 (1994).
16. Radzicka, A. & Wolfenden, R. *Science* **267**, 90–93 (1995).
17. Rini, J. M., Schulze-Gahmen, U. & Wilson, I. A. *Science* **255**, 959–965 (1992).
18. Benkovic, S. J., Adams, J. A., Borders, C. L. Jr, Janda, K. D. & Lerner, R. A. *Science* **250**, 1133–1139 (1990).
19. Tramontano, A., Janda, K. D. & Lerner, R. A. *Science* **234**, 1566–1570 (1986).
20. Hilvert, D., Carpenter, S. H., Nared, K. D. & Auditor, M.-T. M. *Proc. natn. Acad. Sci. U.S.A.* **85**, 4953–4958 (1988).
21. Jacobs, J., Schultz, P. G., Sugawara, R. & Powell, M. *J. Am. chem. Soc.* **109**, 2174–2176 (1987).
22. Cochran, A. G. & Schultz, P. G. *Science* **240**, 781–783 (1990).
23. Janda, K. D., Benkovic, S. J. & McLeod, D. A. *Tetrahedron* **47**, 2503–2506 (1991).
24. Iwabuchi, Y. et al. *J. Am. chem. Soc.* **116**, 771–772 (1994).
25. Reymond, J.-L., Janda, K. D. & Lerner, R. A. *Angew. Chem. int. Edn. engl.* **30**, 1711–1713 (1991).
26. Pollack, S. J., Jacobs, J. W. & Schultz, P. G. *Science* **234**, 1570–1573 (1986).
27. Napper, A. D., Benkovic, S. J., Tramontano, A. & Lerner, R. A. *Science* **237**, 1041–1043 (1987).
28. Campbell, D. A. et al. *J. Am. chem. Soc.* **116**, 2165–2166 (1994).
29. Iverson, B. L., Cameron, K. E., Jahangiri, G. K. & Pasternak, D. S. *J. Am. chem. Soc.* **112**, 5320–5323 (1990).
30. Shokat, K. M., Leumann, C. J., Sugawara, R. & Schultz, P. G. *Nature* **338**, 269–271 (1989).
31. Janda, K. D., Benkovic, S. J. & Lerner, R. A. *Science* **244**, 437–440 (1989).
32. Tramontano, A., Ammann, A. A. & Lerner, R. A. *J. Am. chem. Soc.* **110**, 2282–2286 (1988).
33. Gibbs, R. A., Benkovic, P. A., Janda, K. D., Lerner, R. A. & Benkovic, S. J. *J. Am. chem. Soc.* **114**, 3528–3534 (1992).
34. Martin, M. T., Napper, A. D., Schultz, P. G. & Rees, A. G. *Biochemistry* **30**, 9757–9761 (1991).
35. Lewis, C., Krämer, T., Robinson, S. & Hilvert, D. *Science* **253**, 1019–1022 (1991).
36. Ashley, J. A., Lo, C.-H. L., McElhaney, G. P., Wirsching, P. & Janda, K. D. *J. Am. chem. Soc.* **115**, 2515–2516 (1993).
37. Jacobsen, J. R., Prudent, J. R., Kochersperger, L., Yonkovich, S. & Schultz, P. G. *Science* **256**, 365–367 (1992).
38. Jacobsen, J. R. & Schultz, P. G. *Proc. natn. Acad. Sci. U.S.A.* **91**, 5888–5892 (1994).
39. Cochran, A. G., Pham, T., Sugawara, R. & Schultz, P. G. *J. Am. chem. Soc.* **113**, 6670–6672 (1991).

SUPPLEMENTARY INFORMATION. Requests should be addressed to Mary Sheehan at the London editorial office of *Nature*.

ACKNOWLEDGEMENTS. We thank A. J. Kirby for very helpful discussions during the preparation of this manuscript, and for his independent insights which inspired our analysis. J.D.S. was supported by the Camille and Henry Dreyfus Foundation (1994–99).

## Possible role of climate in the collapse of Classic Maya civilization

David A. Hodell\*, Jason H. Curtis\* & Mark Brenner†

\* Department of Geology, University of Florida, Gainesville, Florida 32611, USA

† Department of Fisheries and Aquatic Sciences, University of Florida, Gainesville, Florida 32653, USA

**THE Maya civilization developed around 3,000 years ago in Mesoamerica, and after flourishing during the so-called Classic period, it collapsed around 750–900 AD<sup>1</sup>. It has been speculated<sup>2–6</sup> that climate change may have played a part in this collapse. But efforts to reconstruct the last three millennia of Mesoamerican climate using palynological methods have met with equivocal success, because human-mediated deforestation has altered regional vegetation in ways that mimic climate shifts, making it difficult to discriminate between natural and anthropogenic changes<sup>7–15</sup>. Here we use temporal variations in oxygen isotope and sediment composition in a 4.9-m sediment core from Lake Chichancanab, Mexico, to reconstruct a continuous record of Holocene climate change for the central Yucatan peninsula. The interval between 1,300 and 1,100 yr BP (AD 800–1,000) was the driest of the middle to late Holocene epoch, and coincided with the collapse of Classic Maya civilization. This continuous climate proxy record thus provides evidence of climate deterioration in the Maya region during the terminal Classic period.**

We investigated the sediment record of Lake Chichancanab (Fig. 1), the largest closed-basin lake in Yucatan, Mexico<sup>16</sup>. ‘Chichancanab’ means ‘little sea’ in Yucatec Maya, which is an appropriate name in view of the lake’s sulphate-rich (2,545 mg l<sup>-1</sup>), high-salinity waters (total dissolved solids,

4,000 mg l<sup>-1</sup>). Today, lake water is at or near saturation with respect to both calcite (CaCO<sub>3</sub>) and gypsum (CaSO<sub>4</sub>). Although gypsum does not precipitate in the open lake today, gypsum crystals are found in littoral areas and at depth in sediments. Past variations in the saturation state of Lake Chichancanab’s water with respect to calcite and gypsum are reflected by changes in the relative proportion of these minerals in the sediment. We assume that downcore shifts in the relative abundance of calcite and gypsum in sediments reflect changes in the hydrologic budget of the lake that were ultimately controlled by changes in the ratio between evaporation and precipitation (E/P).

Regional climate today is characterized by a mean annual temperature of 25.4 °C and yearly rainfall of 1,300 mm, with a rainy season extending from May to September and a dry season from October to April<sup>16,17</sup>. Lake evaporation during the dry season is considerable, and controls the oxygen isotopic composition of Lake Chichancanab’s waters. The average oxygen-isotope composition ( $\delta^{18}\text{O}$ ) of lake water in 1993 was 3.24‰, which is slightly less than the range of 3.4 to 5.4‰ reported in 1973<sup>16</sup>. The lake water is isotopically heavier than the long-term average  $\delta^{18}\text{O}$  of precipitation for the region (weighted mean, -4.0‰)<sup>18</sup>. In 1973,  $\delta^{18}\text{O}$  values of rain and spring water at Chichancanab were -6.1‰ and -4.7‰, respectively<sup>16</sup>. H<sub>2</sub><sup>18</sup>O enrichment in lake water relative to precipitation and ground water reflects evaporative loss of H<sub>2</sub><sup>16</sup>O from the lake<sup>16</sup>. Past changes in the  $\delta^{18}\text{O}/\delta^{16}\text{O}$  ratio of lake water are recorded in the  $\delta^{18}\text{O}$  of carbonate in gastropod and ostracod shells preserved in lake sediments.

We used the oxygen-isotope signal in shell carbonate and the gypsum/calcite ratio in the sediments to reconstruct past changes in E/P. Our working assumption is that times of high E/P (that is, dry climate) are reflected by increased  $\delta^{18}\text{O}$  values of shell carbonate and an increased proportion of gypsum to calcite in sediments. Conversely, periods of low E/P (that is, wetter climate) are marked by low  $\delta^{18}\text{O}$  values and a decreasing proportion of gypsum to calcite.

Near the base of the core, earlier than 8,200 yr before present (BP), a terrestrial environment is indicated by the presence of

land snails (for example, *Gastrocopta* (Pupillidae) and *Cecilioides*; F. Thompson, personal communication) (Fig. 2). Covich<sup>19</sup> also reported the occurrence of terrestrial gastropods before 8,000 yr BP in a core from the southern basin of Lake Chichancanab (that is, Lake Esmeralda, Fig. 1). Both basins were dry during the late Glacial and earliest Holocene, consistent with evidence for lowered water tables and aridity at many sites in the lowland neotropics<sup>20–28</sup>. At 8,200 yr BP, filling of the lake basin is marked by the onset of gypsum precipitation (Fig. 2). A 7-cm-thick charcoal layer occurs just above the increase in sulphur concentration, and is dated directly at  $7,560 \pm 35$  yr BP or between 7,920 and 7,790 yr BP using the 'terrestrial' regression equation (Table 1). The relatively high  $\delta^{13}\text{C}$  of the charcoal (mean,  $-14.4\text{‰}$ ) indicates that it was derived from C<sub>4</sub> vegetation. Microscopic examination of carbonized stem and root fragments suggests remains of burned grasses (L. Newsom, personal communication). Increases in charcoal abundance near the Pleistocene/Holocene boundary have been reported elsewhere in Central America, and are attributed to either natural or human-induced fires<sup>27,30</sup>.

Immediately above the charcoal layer, from 7,750 to 7,260 yr BP, sediments contain abundant, well-preserved tests of the benthic foraminifer *Ammonia beccarii* (Fig. 2). Covich<sup>19</sup> also reported *A. beccarii* at 400 cm in a core from the southern basin of Chichancanab. Although most species of benthic foraminifera are exclusively marine, *A. beccarii* tolerates a wide range of temperatures (10–35 °C) and salinities (7–67 parts per thousand, p.p.t.), but reproduces only at salinities between 13 and 40 p.p.t. (ref. 31). The presence of *A. beccarii* between 7,750 and 7,260 yr BP indicates that the salinity of Chichancanab was higher than today's value of 4 p.p.t. Furthermore,  $\delta^{18}\text{O}$  values of ostracods and gastropods are enriched between 7,800 to 7,200 yr BP, indicating high E/P conditions (Fig. 2).

Lake filling at ~8,200 yr BP was related to sea level rise during the last deglaciation. As sea level rose, so did the level of the freshwater aquifer in Yucatan<sup>16,19</sup>. The filling of Lake Chichancanab occurred during the latter part of the second stage of deglaciation that began at 10,000 yr BP<sup>32</sup> and lasted until 7,000–6,000 yr BP. The rapid rise in lake level occurred ~7,200 yr BP, when calcite precipitation replaced gypsum deposition and  $\delta^{18}\text{O}$  values of ostracods and gastropods decreased abruptly (Fig. 2). Sea level continued to rise slowly after 6,000 yr BP, but the rate was insufficient to substantially affect lake level during the Middle to Late Holocene.

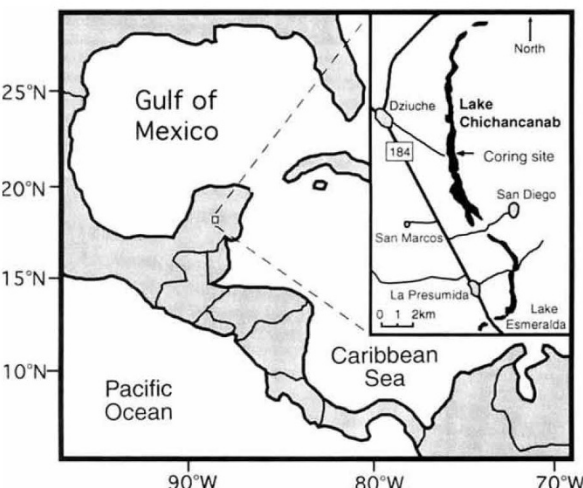


FIG. 1 Map of Central America; inset shows the location of Lake Chichancanab ( $19^{\circ} 50' \text{N}$ ,  $88^{\circ} 45' \text{W}$ , elevation ~15 m above m.s.l.), Yucatan, Mexico. A 4.9-m core was retrieved in 6.9 m of water from the central basin of Chichancanab using a square-rod piston corer and sediment-water interface corer. The core was dated by radiocarbon measurements on charcoal, seed and shell material (Table 1).

TABLE 1 Age analysis of sediment core from Lake Chichancanab

Sample type	Depth (cm)	Accession* number	Age (yr)	Error (±yr)
Terrestrial:				
Seed	65	OS-3545	1,140	35
Charcoal	421	OS-2157	7,560	35
Charcoal	421	CAMS-12780	7,600	60
Charcoal	421	CAMS-12781	7,460	60
Land snail	472	OS-2052	9,180	50
Aquatic:				
<i>Pyrgophorus</i>	15	CAMS-12900	1,550	60
<i>Pyrgophorus</i>	65	OS-3443	1,600	30
<i>Pyrgophorus</i>	103	OS-3446	3,200	40
Bivalves	142	OS-2148	5,210	30
<i>Pyrgophorus</i>	238	OS-3445	7,100	30
<i>Pyrgophorus</i>	314	OS-3444	9,040	65
Mixed gastropods	350	OS-2051	8,680	45
Mixed gastropods	385	OS-2729	9,530	60
Bivalves	406	OS-2055	9,500	50

Radiocarbon analyses were performed on both 'aquatic' shells and 'terrestrial' material (seed, charcoal, land snail) from the Chichancanab core. Because of Lake Chichancanab's hard water, radiocarbon dates on 'aquatic' shells are artificially old (that is, older than their true radiocarbon age) because shells incorporate  $^{14}\text{C}$ -deficient carbon derived from dissolution of local limestone. In contrast, 'terrestrial' materials are immune to the vagaries of hard-water-lake error because they derive their carbon from atmospheric  $\text{CO}_2$ . The age-depth regression equations for aquatic and terrestrial materials are: aquatic, age =  $22.271$  (depth) +  $1,163$  ( $r=0.979$ ); terrestrial, age =  $18.921$  (depth) -  $62$  ( $r=0.998$ ). These regression lines have nearly the same slope and indicate a linear sedimentation rate of  $\sim 0.5 \text{ mm yr}^{-1}$ . The y-intercept for the 'aquatic' regression line suggests a modern hard-water-lake error of  $\sim 1,200$  yr. Depths in the core were converted to age using the 'terrestrial' age-depth regression equation that is not affected by hard-water-lake error.

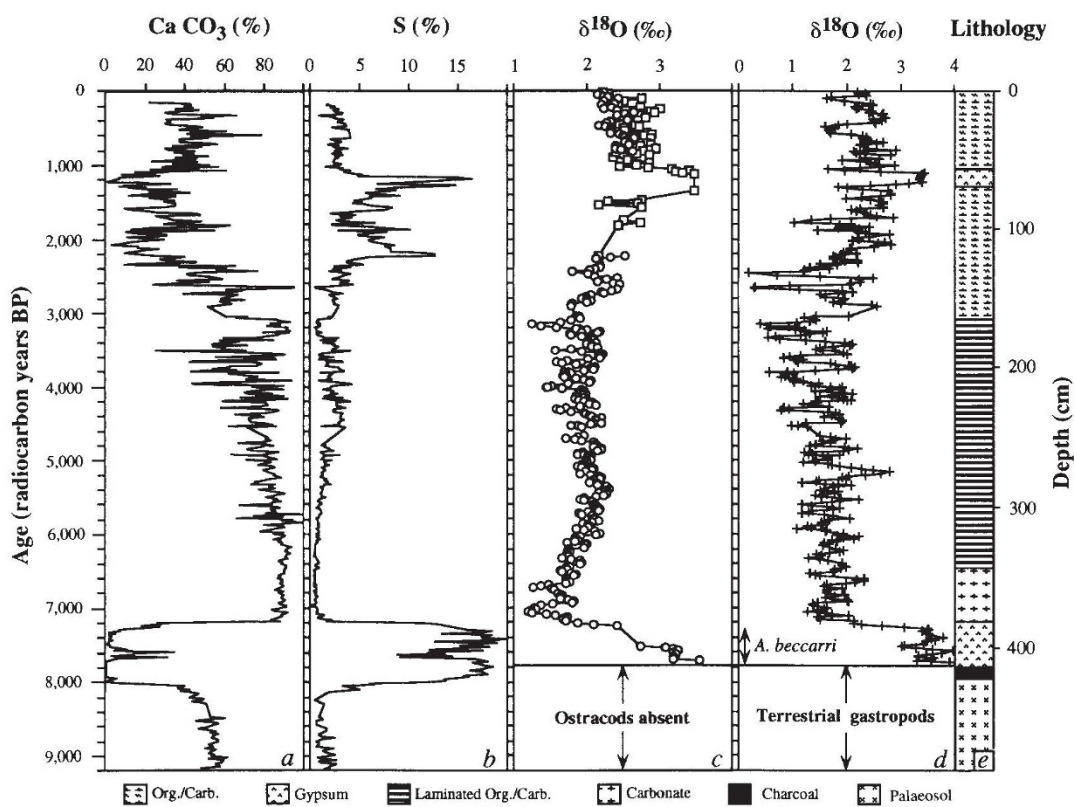
Relatively wet conditions (low E/P) between 7,100 and  $\sim 3,000$  yr BP are indicated by high calcite and low sulphur contents of the sediment, and relatively low  $\delta^{18}\text{O}$  values (Fig. 2). This interval coincides with the Early to Middle Holocene moist period that has been documented elsewhere in the neotropics<sup>16,21,24,29,33,34</sup>. Hodell *et al.*<sup>24</sup> suggested that increased neotropical precipitation during the Early to Middle Holocene was caused by increased intensity of the annual cycle, a consequence of changes in seasonal insolation forced by the Earth's precessional cycle. The inferred climate history from Lake Chichancanab is remarkably similar to that from Lake Miragoane, Haiti, which indicates low lake salinity and moist conditions from  $\sim 7,000$  to  $4,000$  yr BP<sup>24,35</sup>.

During the Late Holocene, climate around the Caribbean Sea became drier relative to the wetter period that prevailed during the Early to Middle Holocene. About 3,000 yr BP, carbonate content of the sediments began to decrease and  $\delta^{18}\text{O}$  values of ostracods started to increase, suggesting the inception of a drying trend (Fig. 2). The interval from 2,200 to 1,200 yr BP was marked by relatively high sulphur content and increasing  $\delta^{18}\text{O}$  values, indicating distinctly drier conditions (Fig. 2). A similar period of exceptionally dry climate was reported from Lake Miragoane between 2,500 and 1,500 yr BP<sup>24,35</sup>. The dry period at Lake Miragoane apparently occurred 300 yr earlier than at Chichancanab, but the difference in timing may be attributed to underestimation of the magnitude of hard-water-lake dating error in Lake Miragoane<sup>35</sup>.

The driest climate conditions occur between  $\sim 1,300$  and  $1,100$  yr BP, reaching a maximum value at  $1,140 \pm 35$  yr BP (Fig. 2). The dating of peak aridity is based on radiocarbon analysis of a seed from 65 cm depth in the core (Table 1). Radiocarbon ages were converted to calendar years using the programme CALIB<sup>36</sup> and the decadal tree-ring dataset<sup>37</sup>, yielding an age range of  $\sim \text{AD } 800$ –1,000 for the arid period with the peak occur-

FIG. 2 The core from Lake Chichancanab was sampled at 1-cm intervals for measurement of  $\text{CaCO}_3$  content (a), total sulphur content (b) and  $\delta^{18}\text{O}$  values of ostracods (c) and the gastropod *Pyrgophorus coronatus* (d). (The  $\delta^{18}\text{O}$  values are w.r.t. the PDB standard.) Oxygen-isotope data were smoothed using a three-point running mean. Because of variable abundance and preservation of ostracods, it was necessary to measure two species for stable isotopes. Circles represent measurements of *Cyprina ophthalmica* and squares represent *Cyprinotus cf. salinus*<sup>41</sup>. The overlap of these species near the top of the core indicates little oxygen-isotope offset between species. The stratigraphic range of the benthic foraminifer *Ammonia beccarii* is shown in d. This zone is underlain by a 7-cm-thick charcoal horizon, and sediments at and below

this level are devoid of ostracods and aquatic gastropods indicating a terrestrial environment. Column e shows the general lithology of the section. Two periods of particularly dry climate (high E/P) are marked by coincident peaks of sulphur content (gypsum) and  $\delta^{18}\text{O}$  values of



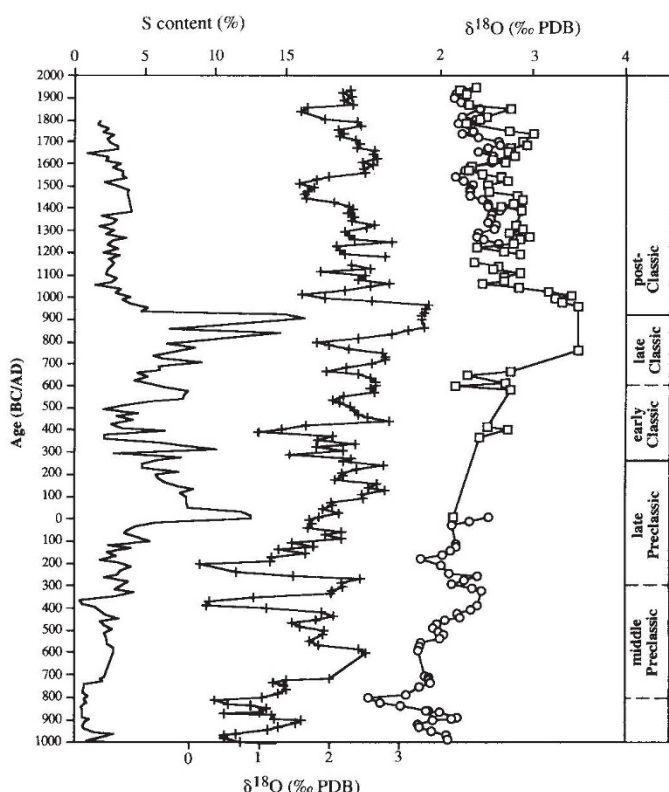
ring at AD 922 (Fig. 3). The timing of this climate drying corresponds approximately to the collapse of the Classic Maya civilization between AD 750 and 900<sup>1</sup>.

Although others have suggested that drought may have played a role in the Classic Maya collapse<sup>2–6</sup>, results from Lake Chichancanab provide the first unambiguous evidence for climate drying between AD 800 and 1000. The continuous Holocene record from Chichancanab sets this event within a long-term climate context. Aside from the period between 8,000 and 7,200 yr BP, when the lake was filling, aridity between 1,300 and 1,100 yr BP (AD 800–1000) represents the driest episode of the past 8,000 yr (Fig. 2).

The palaeoclimate record from Lake Chichancanab alone cannot support the case for regional late Classic drying, but reported low lake stands in central Mexico between 1400 and 900 yr BP<sup>38</sup> and increased fires in Costa Rica<sup>39</sup> may mark the same climate shift<sup>40</sup>. Although the sediment record from Chichancanab suggests a causal link between climate and the late Classic collapse, the region inhabited by the Maya was geologically, ecologically and climatically diverse. The response of climate to any single forcing factor may not have been the same throughout the Mayan region, and so the pattern of cultural change may not

FIG. 3 Sulphur content and three-point running average of  $\delta^{18}\text{O}$  values plotted versus calendar years to 1000 ac. Proxy signals of palaeoclimate (E/P) are compared with major subdivisions of Maya cultural evolution. Symbols are the same as in Fig. 2. The peaks in total sulphur content and  $\delta^{18}\text{O}$  values are centred at ~AD 900 and indicate increased aridity during the terminal Classic period.

both ostracods and gastropods. The first occurs between 8,000 and 7,200 yr BP during the Early Holocene, and the second is centred at 1,200 yr BP during the Late Holocene.



have been uniform. For example, the collapse seems to have been strongest in the southern Maya lowlands with populations shifting to the north<sup>1</sup>. Even if the drying were regional in extent, however, the ecological and anthropological effects could have varied spatially, depending on the magnitude of subregional climate change and the sensitivity of the natural and cultural systems to environmental change. Further study is needed to determine the full magnitude and geographical extent of the dry period that occurred between AD 800 and 1000, and to explain the intraregional pattern of the collapse of Classic Maya civilization. □

Received 11 January; accepted 25 April 1995.

1. Lowe, J. W. G. *The Dynamics of Apocalypse* (Univ. New Mexico Press, Albuquerque, 1985).
2. Gunn, J. & Adams, R. E. W. *Wild Archaeol.* **13**, 87–100 (1981).
3. Folan, W. J. & Hyde, B. H. in *Contributions to the Archaeology and Ethnohistory of Greater Mesoamerica* (ed. Folan, W. J.) 15–48 (Southern Illinois Univ., Carbondale, 1985).
4. Folan, W. J., Gunn, J., Eaton, J. D. & Patch, R. W. *Archaeology* **10**, 454–468 (1983).
5. Messenger, L. C. Jr *Ancient Mesoamerica* **1**, 21–40 (1990).
6. Dahlin, B. H. *Clim. Change* **5**, 245–263 (1983).
7. Deevey, E. S. *Pol. Arch. Hydrobiol.* **25**, 117–129 (1978).
8. Deevey, E. S. *et al. Science* **206**, 298–306 (1979).
9. Vaughan, H. H., Deevey, E. S. & Garrett-Jones, S. E. in *Prehistoric Lowland Maya Environment and Subsistence Economy* (ed. Pohl, M. D.) 73–89 (Harvard Univ., Cambridge, 1985).
10. Wiseman, F. M. in *Prehistoric Lowland Maya Environment and Subsistence Economy* (ed. Pohl, M. D.) 63–71 (Harvard Univ., Cambridge, 1985).
11. Higuera-Gundy, A. in *Biogeography of the West Indies: Past, Present, and Future* (ed. Woods, C. A.) 191–200 (Sandhill Crane, Gainesville, 1989).
12. Wiseman, F. M. in *Ancient Maya Wetland Agriculture: Excavations on Albion Island, Northern Belize* (ed. Pohl, M. D.) 312–322 (Westview, Boulder, 1990).
13. Hansen, B. C. S. in *Ancient Maya Wetland Agriculture: Excavations on Albion Island, Northern Belize* (ed. Pohl, M. D.) 155–186 (Westview, Boulder, 1990).
14. Higuera-Gundy, A. thesis, Univ. Florida (1991).
15. Bradbury, J. P., Forester, R. M., Bryant, W. A. & Covich, A. P. in *Ancient Maya Wetland Agriculture: Excavations on Albion Island, Northern Belize* (ed. Pohl, M. D.) 119–154 (Westview, Boulder, 1990).
16. Covich, A. & Stuiver, M. *Limnol. Oceanogr.* **19**, 682–691 (1974).
17. Garcia, E. *Publ. Inst. Geogr. Univ. Nac. Aut. Mex.* **1**, 173–191 (1965).
18. Rozanski, K., Araguás-Araguás, L. & Gonfiantini, R. in *Climate Change in Continental Isotopic Records* (eds Swart, P. K., Lohmann, K. C., McKenzie, J. & Savin, S.) 1–36 (Am. Geophys. Union, Washington DC, 1993).
19. Covich, A. P. thesis, Yale Univ. (1970).
20. Watts, W. A. *Geology* **3**, 344–346 (1975).
21. Bradbury, J. P. *et al. Science* **214**, 1299–1305 (1981).
22. Markgraf, V. *Quat. Sci. Rev.* **8**, 1–24 (1989).
23. Bush, M. & Colinvaux, P. A. *J. Veget. Sci.* **1**, 105–118 (1990).
24. Hodell, D. A. *et al. Nature* **352**, 790–793 (1991).
25. Bush, M. B. *et al. Ecol. Monogr.* **62**, 251–275 (1992).
26. Watts, W. A., Hansen, B. C. S. & Grimm, E. C. *Ecology* **73**, 1056–1066 (1992).
27. Leyden, B. W., Brenner, M., Hodell, D. A. & Curtis, J. H. in *Climate Change in Continental Isotopic Records* (eds Swart, P. K., Lohmann, K. C., McKenzie, J. & Savin, S.) 165–178 (Am. Geophys. Union, Washington DC, 1993).
28. Leyden, B. W., Brenner, M., Hodell, D. A. & Curtis, J. H. *Palaeogeogr. Palaeoclimatol. Palaeoecol.* **109**, 193–210 (1994).
29. Piperno, D. R., Bush, M. B. & Colinvaux, P. A. *Quat. Res.* **33**, 108–116 (1990).
30. Emiliani, C., Price, D. A. & Seipp, J. in *Stable Isotope Geochemistry: A Tribute to Samuel Epstein* (eds Taylor, H. P., O'Neil, J. R. & Kaplan, I. R.) 229–231 (Geochemical Soc., San Antonio, 1991).
31. Bradshaw, J. S. *J. Paleontol.* **31**, 1138–1147 (1957).
32. Fairbanks, R. G. *Nature* **342**, 637–642 (1989).
33. Leyden, B. W. *Proc. natn. Acad. Sci. U.S.A.* **81**, 4856–4859 (1984).
34. Leyden, B. W. *Ecology* **66**, 1279–1295 (1985).
35. Curtis, J. C. & Hodell, D. A. in *Climate Change in Continental Isotopic Records* (eds Swart, P. K., Lohmann, K. C., McKenzie, J. & Savin, S.) 135–152 (Am. Geophys. Union, Washington DC, 1993).
36. Stuiver, M. & Reimer, P. J. *Radiocarbon* **35**, 215–230 (1993).
37. Stuiver, M. & Becker, B. *Radiocarbon* **35**, 35–65 (1993).
38. Metcalfe, S. & Hales, P. *Mem. Calif. Acad. Sci.* **17**, 501–515 (1994).
39. Horn, S. & Sanford, R. L. *Biotropica* **24**, 354–361 (1992).
40. Street Perrott, F. A. *Ambio* **23**, 37–43 (1994).
41. Price, L. G. thesis, Washington Univ. (1974).

**ACKNOWLEDGEMENTS.** We thank F. Thompson for identifying molluscs, L. Newsom for identifying carbonized plant fragments, and K. Venz for providing laboratory assistance; B. Curtis, M. Hart, R. Medina, M. Mulligan and C. Ullmann for field assistance; and M. Kashgarian and G. Jones for providing radiocarbon dates. Reconnaissance at Chichancanab in 1992 was supported by a NASA grant to B. Dahlin. We thank the Instituto de Antropología e Historia (INAH) for cooperative support and F. A. Street-Perrott for a thoughtful review. This work was supported by NOAA.

## Young peridotitic diamonds from the Mir kimberlite pipe

N. Shimizu\* & N. V. Sobolev†‡

\* Department of Geology and Geophysics,  
Woods Hole Oceanographic Institution, Woods Hole,  
Massachusetts 02543, USA

† Institute of Mineralogy and Petrography, Siberian Branch,  
Russian Academy of Sciences, Novosibirsk, Russia

‡ Department of Geology, Union College, Schenectady,  
New York 12308, USA

MINERAL inclusions in diamonds contained in the explosive volcanic rocks known as kimberlites provide an important record of geochemical processes in the continental lithosphere. Samarium–neodymium model ages as old as 3.2 Gyr have been obtained for many peridotitic mineral inclusions<sup>1–4</sup>, pointing to the great antiquity of the host ‘peridotitic’ diamonds (relative to the age of the associated kimberlites) and hence an extended period of residence in the sub-continental mantle. Here we report trace-element data from garnet inclusions in peridotitic diamonds from the Mir kimberlite pipe, Siberia, which appear to be inconsistent with this interpretation. The heterogeneous distribution of the trace elements both within and among discrete garnets from single diamonds are indicative of rapid crystal growth leading to solid-melt disequilibrium on a local scale. The conditions for survival of these heterogeneities within individual garnet crystals are tightly constrained by diffusion kinetics, which would rapidly homogenize the trace-element distributions in the sub-continental mantle. Thus, while it seems clear that peridotitic diamonds and their inclusions are derived from ancient lithospheric material, our data require that they crystallized shortly before the eruption of the kimberlite 360 Myr ago<sup>5</sup>.

Samples examined here are chrome pyrope garnets from three diamonds from the Mir kimberlite pipe, Siberia. All three diamonds were colourless, sharp-edged, slightly flattened octahedral crystals typical of the Yakutian diamond deposits<sup>6</sup>. No cracks were observed in any parts of the crystals, and no morphological modifications indicative of crack-healing/overgrowth were present. The initial weights of the crystals were 0.2, 0.24 and 0.9 carats for MR92/9, MR129/15 and AV49, respectively. Six discrete garnet grains from MR92/9, a large (200 × 200 × 200 µm) grain from MR129/15, and five grains from AV49 were liberated from host diamonds by burning them individually in a platinum bucket in air at 800 °C for several hours. Samples were optically examined occasionally during the procedure and liberated garnet grains were removed from the bucket. Cracks (depicted in Fig. 2) were probably induced by differential thermal expansion of the inclusion and host during liberation. Although no further studies were made on the host diamonds before liberation of inclusions, we assert that the integrity of the stones is beyond any doubt and strongly believe that the chemical characteristics reported here can be considered primary. Major-element compositions are characterized by low Ca (from 1.3 wt% CaO in MR129/15 to 2.6 wt% in AV49) and high Cr (from 7.9 wt% Cr<sub>2</sub>O<sub>3</sub> in MR129/15 to 11.8 wt% in MR92/9), consistent with the general characteristics of diamond inclusion garnets of the peridotite suite<sup>7</sup> of clinopyroxene-free<sup>8</sup> dunite-harzburgite paragenesis<sup>9</sup>. Rare-earth elements (La, Ce, Nd, Sm, Eu, Dy, Er, Yb), Ti, V, Sr, Y and Zr were determined with a Cameca IMS 3f ion microprobe at Woods Hole Oceanographic Institution using techniques described elsewhere<sup>10</sup>. Analytical uncertainties involved in the present dataset are 10–20% for rare-earth elements (REE) and 5–10% for other trace elements.

Figure 1 illustrates REE variations within and among discrete garnets. There are two salient features of the data. First, general similarities exist among grains from a single diamond host. For instance, six grains from MR92/9 share strong depletion in light